JPMTR 067 | 1430
DOI 10.14622/JPMTR-1430
UDC 003.29 : 004.93/7.061

Research paper
Received: 2014-07-30
Accepted: 2015-07-26

Image analysis as a tool to discriminate counterfeit from true 2D printed codes

Nadège Reverdy-Bruas, Lionel Chagas, Jean-Pascal Poletti, Raphaël Passas

Univ. Grenoble Alpes, LGP2, F-38000 Grenoble, France
CNRS, LGP2, F-38000 Grenoble, France
Agefpi, LGP2, F-38000 Grenoble, France

E-mail: nadege.reverdy@pagora.grenoble-inp.fr
lionel.chagas@pagora.grenoble-inp.fr

Abstract

The general context of this study is to establish recommendations for the development of digital models in the framework of counterfeiting. To achieve this goal, printed 2D codes were investigated. Visual Basic tools have been developed in order to automate tasks. The present paper allows characterizing the printing process used (conventional and waterless offset); sensitive results were also obtained regarding the kind of printed substrate (coated and uncoated paper). Histograms of area classes were plotted and they revealed that the printing process induced the raise of a new class of small dots not present on the digital file. In addition, two types of counterfeiting methods were carried out and they pointed out that the histograms of the counterfeit codes were different from the original printed code, whatever the attempt of counterfeiting. Furthermore, in these cases, small dots tend to agglomerate and form new area classes of bigger size. The method developed in this study thus allows the identification of the printing process as well as the distinction of true and counterfeit 2D codes.

Keywords: 2D codes, counterfeiting, security, automation, image analysis

1. Introduction and background

The general context of this study is to establish recommendations for the development of digital models in the framework of counterfeiting (Jotcham, 2005). The first step of the research was to characterize the similarity between a printed 2D code and the corresponding numerical file (Chagas et al., 2013). The present article summarizes the second phase of characterization of 2D printed codes.

Even if they are similar to stacked 1D barcodes, 2D codes work in a very different way. They require a 2D scanner to be read, consisting of a camera – generally a smartphone – that acquires a picture of the substrate. In a second step, the picture is analysed for the purpose of restoring the original code and decrypting the information contained in it. These steps require complex mathematical treatment to be applied on the picture (Chu et al., 2011; Wang and Zou, 2006).

In 1994, Denso Wave, a subsidiary of the Japanese company Toyota, developed a 2D code to mark components. This code can be quickly read by cameras, so they can identify and sort the components automatically, quickly and without ambiguity (DENSO WAVE, 2013). It is rightly called QR code – for Quick Response Code – and has been subject to several standards, in particular ISO 18004 in June 2000, after Denso published QR code as a royalty-free license in 1999. This permitted its global expansion and use in various application fields.

7 % redundancy | 30 % redundancy | Stylized | Logo

Figure 1: Various QR code features encoding the same web link

QR code (Figure 1) public success is due to its high-speed readability, high-capacity data storage and reliability (from 7 % to 30 % of redundancy). Moreover it is not only a conveyer of characters as part of numbers or texts, but also contains various kinds of content. It is possible to create QR codes containing business card information, web link, Wi-Fi settings, pre-filled SMS… Free QR code generators are available on internet (UNITAG, 2013). The size of this code depends on the information encoded and the rate of redundancy, which results from Reed-Solomon theory (Swetake, 2013). Thanks to this system, one can integrate logos or drawings into a QR code: even if it hides a part of the code and redundancy is decreased, it is still correctly decodable (Figure 1).

As QR codes are widely used by general public, other 2D codes have been developed such as Data Matrix, for the applications rather industrial than public (Stevenson, 2005). This one was invented in October 2005 by a subsidiary of Siemens. It is similar to a QR code (Figure 2) and uses Reed-Solomon algorithm too. Covered by ISO 16022, Data Matrix can encode various kinds of information (text, web link, SMS…); however, it is mostly used for marking small electronic components. One of the advantages of this code is its readability with a very low contrast – 20 % is sufficient. In addition, Data Matrix has become mandatory on every medicine box since 1st of January 2011 in France (Lemaire, 2011).

Figure 2: Data Matrix encoding a web link to Google

There is also a possibility of encoding information in clustered-dot halftones, a system that uses the properties of this kind of printing in order to avoid black-and-white pixel-like blocks on an advertisement (Ulichney, Gaubatz and Simske, 2010).

The ANR Estampille project, of which this study is a part, fits into a global strategy of prevention and deterrence in regard to the fight against counterfeiting. In this context there are two key concepts to take into account: authenticity and traceability.

- The authenticity of a product is the correspondence between its description and its characteristics. Detecting a counterfeit item requires to define relevant characteristics, so that controls can be done in a reasonable time – most of the time they involve technical parameters quickly recognizable. It is important not to confuse identification and authentication: identification helps to visually recognize the protected product (brand, logos, various indications…), whereas authentication consists in checking this identity, the correspondence between the product and the indications.
- Traceability means collecting information – by single product or product batch – about the production stages and location data. Such indication can be consulted on demand but it is not a mean of authentication (anomalies in traceability can still trigger suspicion).

There are a lot of technologies meeting these requirements that are used as security systems. They all have assets and drawbacks, so they have to be chosen regarding the product: target market, difficulty of counterfeiting, cost of implementation, etc.

There are many technologies to secure documents: Cryptoglyph®, microtaggants, geometrical distortion analysis, multilayer stickers, selective varnish, Bokode®, special paper, etc. Among this variety of security systems, 2D codes present the advantage of being really cheap and easy to implement in a production line. Moreover, the large amount of free generators available on the web promotes the global expansion of their use in various domains. But because they are visible and easily printable, they are likely to be counterfeited.

In this context, 2D codes composed of very small modules (down to 10 μm) corresponding to the smallest dots printable at high resolution (up to 2400 dpi) are under development. This parameter makes it really different from classical 2D codes such as QR codes. Table 1 summarizes the orders of magnitude of widely used 1D and 2D codes.

Table 1: Orders of magnitude – storage for selected code sizes – of 1D and 2D codes

Code	Storage capacity	Module size	Code size
1D barcode (EAN-13)	13 digits – 46 bits	1 mm × 15 mm	30 mm × 20 mm
QR code	Up to 7089 digits or 4296 alphanumeric data – 24800 bits	1 mm × 1 mm	20 cm × 20 mm
Data Matrix	Up to 3119 digits or 2335 alphanumeric data – 10900 bits	1 mm × 1 mm	10 mm × 10 mm
High resolution codes	About 60000 bits	20 μm × 20 μm	5 mm × 5 mm

The high resolution codes, discussed in this paper, exhibit a 250 times higher data storage capacity than traditional 2D codes. It is therefore obvious that the challenge is to minimize the module size (and the code size) while keeping the robustness of the code. The small size of the modules makes these kinds of codes nearly impossible to copy.

Therefore, the present study focuses attention on the characterization of 2D codes printed by different printing processes on different substrates and for different resolutions (dot size). The final aim is to point out the reliability of the 2D code after a first print and after a copy. This is performed by studying the histograms of the number of elements in a class of area.

2. Methods

The analyzed codes are made of single dots and groups of dots on matrixes 100 × 100, printed by different printing processes. It is therefore possible to compare the deformation of 2D codes due to the variability of printing parameters: substrate – coated and uncoated, elementary dot size or printing resolution – dot size from 10.2 to 42.4 μm, printing process – conventional and waterless offset; the print area coverage is maintained at the same level (20 %) in this study.

The successive steps carried out to analyse the printed codes consist of:

- developing methods of image analyses by creating macros with VBA (Visual Basic for Applications) on Visolog®,
- choosing an automatic threshold method,
- establishing histograms showing the number of elements in a class of area.

Finally, two counterfeiting strategies were tested:

- a second print of an original printed code after its digitalization,
- a second print from the digitally reconstructed printed code.

2.1 Printing process

In this study, investigations were focused on the prints obtained with waterless offset, and to a small extent, to conventional offset for the original printed code. Then, counterfeit code was printed using a Ricoh electrophotography press.

2.2 Printing substrate

Two kinds of substrates were printed: a coated paper and an offset uncoated paper. Measurements were performed on 10 samples of each kind of paper to characterize their main properties. Table 2 summarizes the results.

The main difference among these two substrates that has a direct impact on the reproduction of the 2D code is the roughness. It is about 0.8 μm for the coated paper and about 6.3 μm for the uncoated one which is typical for these grades.

2.3 Dot size

On the digital test chart, four series of squares of increasing coverage percentages were designed. Each one was printed with a unique printing resolution: 2 400, 1 200, 800 and 600 dots per inch (dpi).

The hardware resolution corresponds to the size of the smallest dot that it can print. A hardware resolution of 2 400 dpi means that it can print dots that are 10.6 μm wide (1 inch = 2.54 cm, 2 400 dots in 1 inch implies that 1 dot measures 2.54/2 400 = 0.00106 cm = 10.6 μm in width). In computer science, the equivalent is the pixel: it is the smallest element that can be displayed by a device (screen). The dimension of the elemental dots in the 2D code varies regarding the printing resolution. It is respectively 10.6, 21.2, 31.8 and 42.4 μm for 2 400, 1 200, 800 and 600 dpi resolutions.

Table 2: Main characteristics of the two studied papers

Paper		Basis weight (g/m²)	Thickness (μm)	Specific volume (cm³/g)	CIE whiteness	PPS Roughness (μm)
Coated paper	**Mean**	88.90	64.00	0.72	118.06	0.78
	Standard deviation	0.20	0.90	0.01	1.03	0.05
Uncoated paper	**Mean**	150.90	169.90	1.13	131.45	6.27
	Standard deviation	0.50	2.40	0.02	0.71	0.08

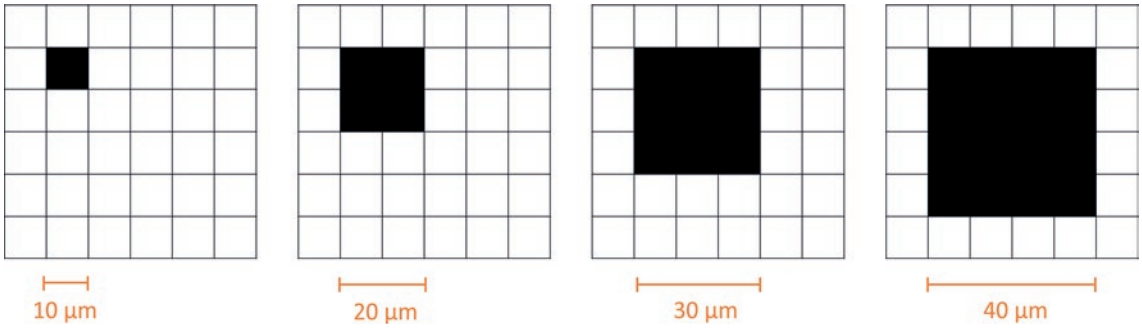

Figure 3: Principle pattern of a 2400 dpi hardware printing a dot at 2400, 1200, 800 and 600 dpi (from left to right) – approximated sizes

A hardware that has a 2400 dpi resolution can also print at lower resolution: in this case, it combines dots at 2400 dpi to have groups of dots that have the size of the desired printing resolution (Figure 3).

2.4 Picture acquisition

2.4.1 Hardware

In order to analyse pictures as clean as possible at very high resolution – and therefore to minimize the influence of the acquisition in the image analysis – the samples were digitalized by an optical Zeiss Microscope Axio Imager.M1m, with associated software Axio Visio, Release 4.8.

2.4.2 Image acquisition protocol

Each printed sample has been digitalized according to the following acquisition protocol on the microscope, to have the same acquisition condition and so to minimize the influence of this step.

- 100-fold magnification (adapted to acquire the smallest squares, printed at 2400 dpi; for the others, it is necessary to make four or nine pictures and combine them into mosaic)
- Reflection light with the highest level of intensity and black background
- Shading process to have an homogeneous light
- Exposure time: 6.40 s
- Pictures: RGB in TIFF format, standard size: 2584 × 1936 pixels

2.5 Image analysis

2.5.1 Software

All the image treatments of the project have been done with Visilog® 7.0, image analysis software of the company Noesis. It is a powerful tool including a lot of functions to analyse complex and even 3D images (VISILOG, 2015). Moreover this software is highly customizable and VBA (Halvorson, 2008) can be used to create macros, in order to improve the protocols of image analysis and to automate a lot of tasks.

Microsoft® Excel® 2013 has been used to gather data of the samples studied and plot graphs.

2.5.2 Surface of interest

In this study, analyses were focused on 100 × 100 pixels matrixes and did not take into account the printed borders in order them not to influence the measurements. Figure 4 shows the targeted area (4b) selected on the picture taken with the microscope (4a).

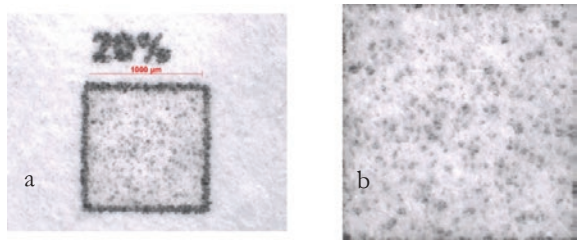

Figure 4: Acquisition of the original picture (a) and corresponding surface of interest (b)

2.5.3 Thresholding

To perform image analysis, binary images are required. It is therefore necessary, from the RGB pictures, to separate the color layers of the image and to threshold one of them. Several thresholding methods can be carried out from the histogram of grey levels.

The manual method consists in creating two value ranges from the color intensity values of each pixel. Pixels which have an intensity value between 0 and the chosen threshold – the darkest – will be converted into black, and pixels which have an intensity value between the chosen threshold and 255 – the brightest – will be converted into white. The threshold can be chosen in regard to the image histogram. Some images clearly show two peaks, so the approximate limit between the peaks is an adapted value for the threshold. When the

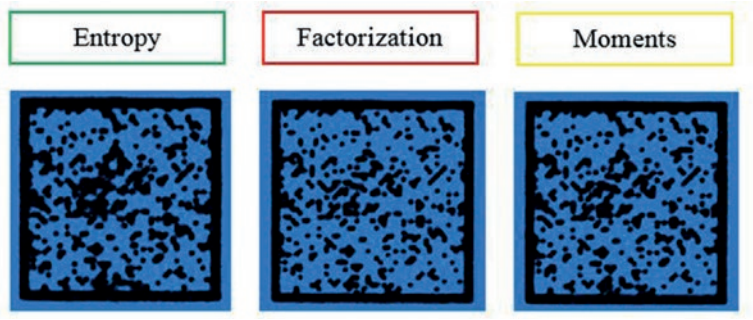

Figure 5: Example of automatic thresholding methods applied on the same 2D code

histogram do not have such appearance, it is more difficult to choose an accurate threshold.

The interactive manual method allows visualizing the result of the thresholding and therefore, the chosen threshold value is adjustable.

Finally, the threshold can be performed automatically using algorithms. Three algorithms available on Visilog® were evaluated: entropy, factorization and moments. The function generates a spreadsheet containing the calculated threshold, depending on the chosen algorithm. An example of pictures obtained using these three methods is depicted in Figure 5.

The visual methods – manual and interactive manual – are not adapted because they do not allow an automation of tasks. The fidelity method (that adjusts the threshold with the known 2D code) implies that the digital file is known. Therefore, it cannot be applied to counterfeiting realized on a printed code.

The factorization method was selected because it was the one that gave, on several tested samples, the best satisfying visual results. Furthermore, it is an automated method allowing carrying out a constant protocol.

2.5.4 Histogram of area distribution

On the binary picture obtained after thresholding, the Visilog® software allows to count the groups of pixels of the same intensity (taking the value 0 or 1 depending on if they represent the inked part or the non-inked part of the code).

2.5.5 Comparison of pictures

In order to compare the printed 2D code to the digital file, a first step is required. Indeed, they must be of the same size. The theoretical picture – 100 × 100 matrix – is a 100 × 100 pixels image, whereas the pictures captured from the microscope have a variable size ranging from 1 000 × 1 000 pixels to 2 500 × 2 500 pixels.

The image from the microscope cannot be resampled, to avoid the loss of information; so it is the theoretical square (extracted from the test chart file) that must be resampled.

There are several methods to achieve this: Photoshop® and Visilog® include functions to resample an image, based on complex algorithms. But they deteriorate the shape of the original pixels, so another method has been developed: decoding and reconstructing the image thanks to a complex macro.

Each pixel of the original 100 × 100 pixels matrix is scanned; the value is stored in an Excel® sheet; a new image of the same size as the sample is created; then the information is reported onto this new image without any deterioration, i.e. the aspect ratio is kept (Figure 6).

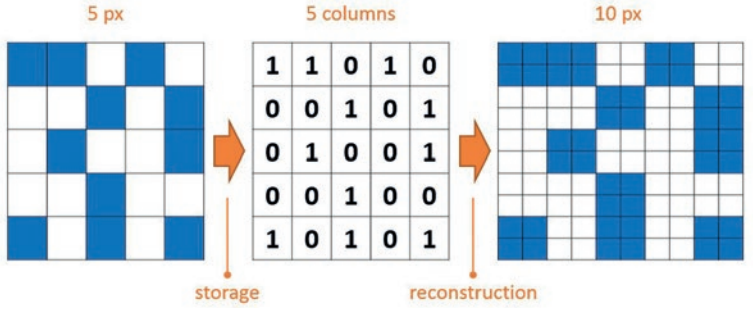

Figure 6: Resampling a theoretical image without any deterioration (px – pixel)

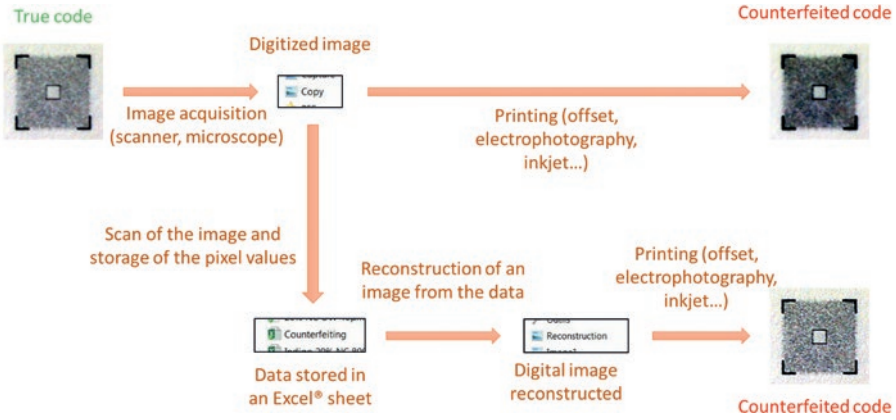

Figure 7: Different steps realized to compare an original print to a second print of a same 2D code – two strategies of counterfeiting studied

2.6 Simulation of counterfeiting – two strategies

2.6.1 General overview

In this part, the possibility to counterfeit a 2D code is studied. Two strategies were considered (Figure 7):

- the direct counterfeiting: second print after digitalization of a printed code,
- the indirect counterfeiting: second print with integration of an intermediate step of reconstructed image.

2.6.2 Image reconstruction

Image reconstruction in the context of counterfeiting has some similarities with the resampling of the theoretical image formerly presented (Chap. 2.5.5. and Figure 6). The major difference is that in counterfeiting, the input image is a 1 000 × 1 000 pixels to 2 500 × 2 500 pixels, and the output image is of the same size. Therefore, it is necessary to resample the input image, but because of the deterioration due to printing and acquisition, the data in the image cannot be easily read.

To decode the information, a method has been developed. It deals with the superimposition of a layer of 100 squares × 100 squares, each square corresponding to 1/(100 × 100) = 0.01 % of the total surface of the image. From there, two parameters are configurable: the square width and the coverage percentage; this parameter corresponds to the coverage percentage of the square from which one can consider that on the corresponding theoretical image, there was a dot (Figure 8). This method scans the entire image, stores the data in an Excel® sheet and then reconstructs an intermediate theoretical image the same way as the former resampling method.

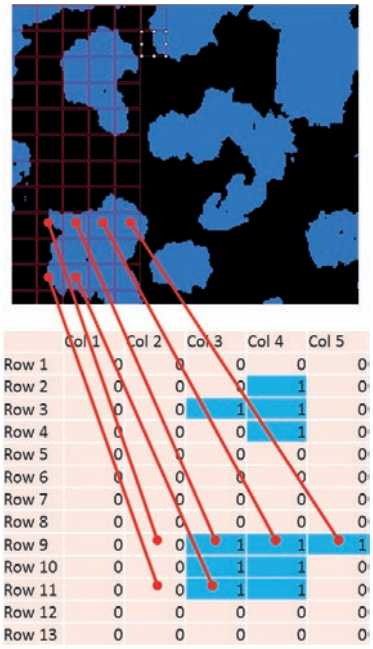

	Col 1	Col 2	Col 3	Col 4	Col 5
Row 1	0	0	0	0	0
Row 2	0	0	0	1	0
Row 3	0	0	1	1	0
Row 4	0	0	0	1	0
Row 5	0	0	0	0	0
Row 6	0	0	0	0	0
Row 7	0	0	0	0	0
Row 8	0	0	0	0	0
Row 9	0	0	1	1	1
Row 10	0	0	1	1	0
Row 11	0	0	1	1	0
Row 12	0	0	0	0	0
Row 13	0	0	0	0	0

Figure 8: Example of decoding a 1 600 × 1 600 pixels image: square width = 90 %, coverage percentage = 95 %

3. Results

As previously mentioned, the thresholding method by factorization was selected. The Visilog® software thus allows analyzing the surface of each element.

On a 1 600 × 1 600 pixels image of 100 modules × 100 modules, if no deterioration due to printing of acquisition would occur, an isolated dot would have a (1 600 × 1 600)/(100 × 100) = 256 pixels surface. This surface A is the reference used for the classification (it depends on the size of the studied sample). On the histograms below (Figures 9–16), X elements in the class N means that there are X elements which surface is in

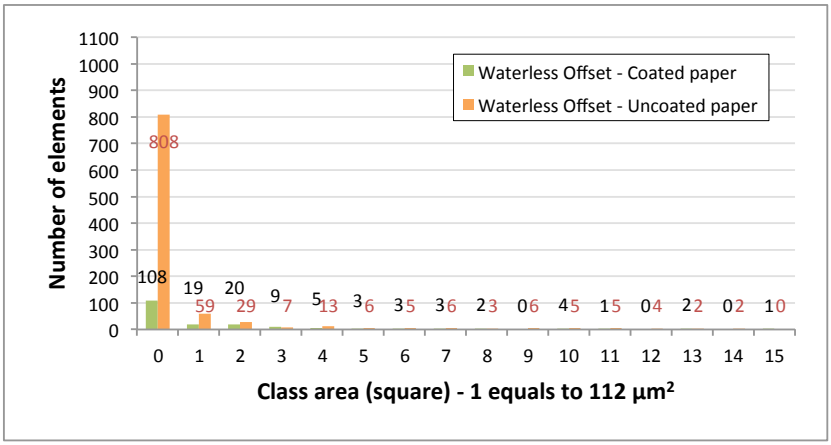

Figure 9: Size distribution histogram of a 2D code – 20 % of coverage, 10.6 µm dot – waterless offset on coated and uncoated paper

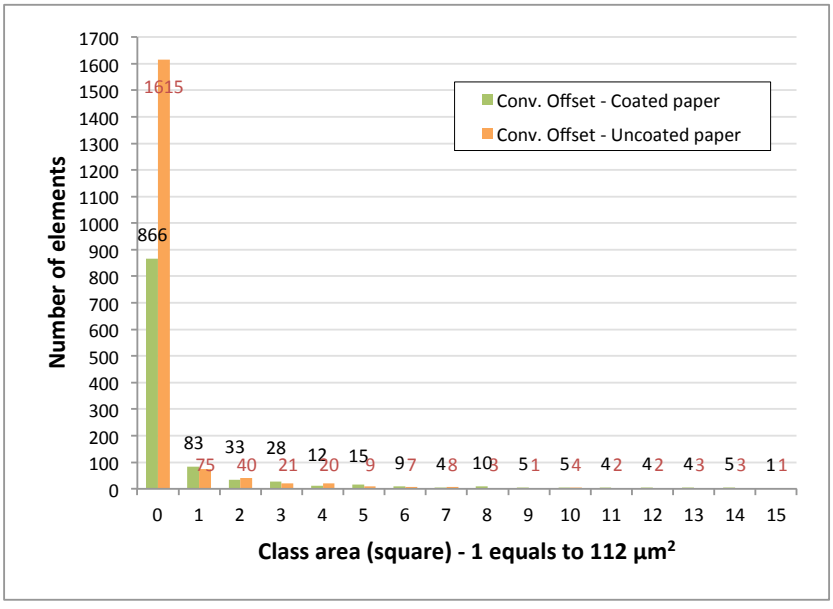

Figure 11: Size distribution histogram of a 2D code – 20 % of coverage, 42.4 µm dot – waterless offset on coated and uncoated paper

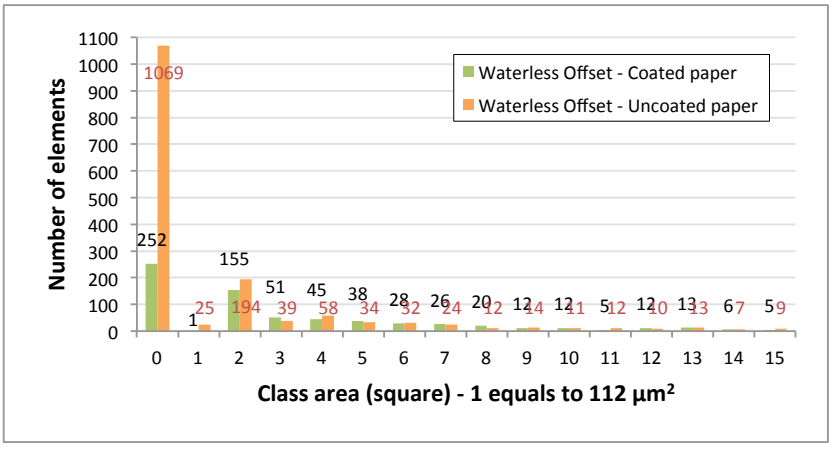

Figure 10: Size distribution histogram of a 2D code – 20 % of coverage, 10.6 µm dot – conventional offset on coated and uncoated paper

the range $[(N - 0.5) \times A; (N + 0.5) \times A]$. The class of surface 0 corresponds to elements which surface is in the range $[0; 0.5 \times A]$.

3.1 Case of the first print

3.1.1 Size distribution histogram of the printed code

Figures 9 and 10 represent the size distribution histogram of a code with a 20 % of coverage, 10.6 µm dots and printed by waterless or conventional offset on coated or uncoated paper, respectively.

From these histograms (Figure 9 and 10), it is important to notice the number of elements in the class 0 that represent the smallest printed elements but that can also be "parasite" dots.

The main key points to underline are:

- the number of elements in the class 0 is far higher for the uncoated paper compared to the coated one whatever the printing process,
- the number of elements in the class 0 is lower for waterless offset (Figure 9) than for conventional offset (Figure 10), whatever the substrate.

A similar analysis was performed for waterless offset with a 42.4 µm dot (Figure 11). The same tendency is observed with the raise of the class 0 and the higher number of elements on the uncoated paper

3.1.2 Size distribution – comparison with the digital file

On Figures 12 and 13 and on Figures 14 and 15, the comparison between printed code and digital file is pointed out for waterless and conventional offset, respectively.

For the digital file, there is no element in the class 0 because the smallest element of the code is a multiple of the basis surface (A); therefore, no element can have a surface size in the range 0 to $0.5 \times A$. With waterless, as well as with conventional offset, and for a 10.6 µm dot, a lot of small elements are generated on the printed code.

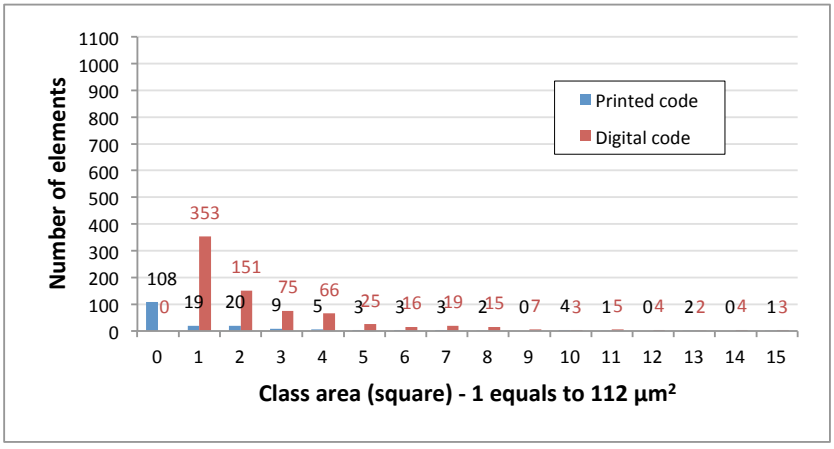

Figure 12: Size distribution of a 2D code – 20 % of coverage, 10.6 µm dot, waterless offset on coated paper – comparison with the digital file

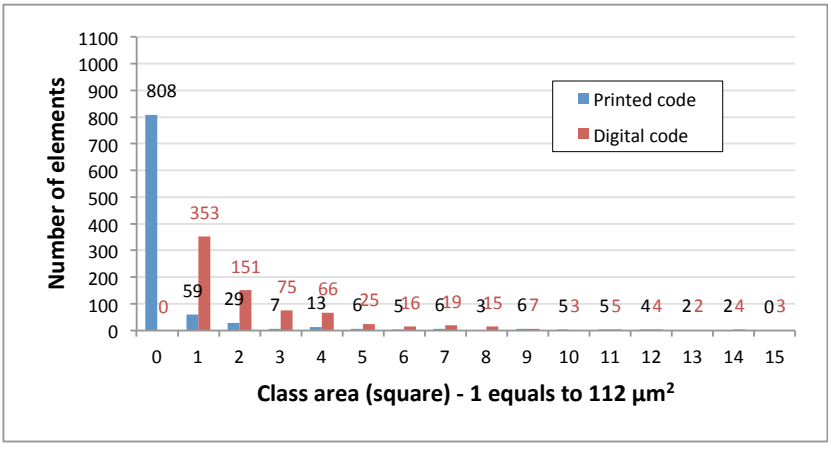

Figure 13: Size distribution of a 2D code – 20 % of coverage, 10.6 µm dot, waterless offset on uncoated paper – comparison with the digital file

3.2 Case of the second print

In order to apply the reconstruction method to the code, samples were printed with a Ricoh electrophotography press for a 20 % of coverage code, on uncoated paper, with dot size of 21.2 µm, 31.8 µm and 42.4 µm. The maximum resolution of the press being 1200 dpi, it was not possible to print 10.6 µm dots. The different cases are depicted on Figure 16. In the class 0, there are more than 3 333 elements for the true code and for the one counterfeit with the direct method (Visilog® cannot analyse more than 3 333 elements). For the counterfeit code with the image reconstruction method, only 1 875 elements are counted.

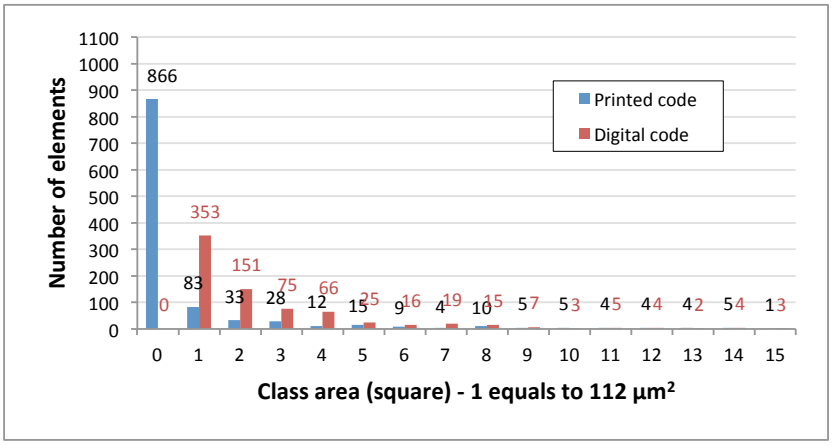

Figure 14: Size distribution of a 2D code – 20 % of coverage, 10.6 µm dot, conventional offset on coated paper – comparison with the digital file

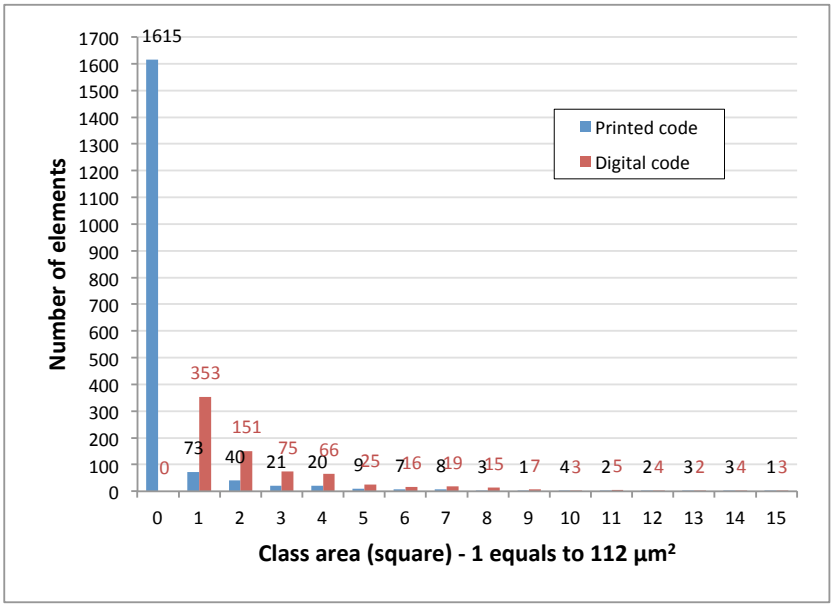

Figure 15: Size distribution of a 2D code – 20 % of coverage, 10.6 µm dot, conventional offset on uncoated paper – comparison with the digital file

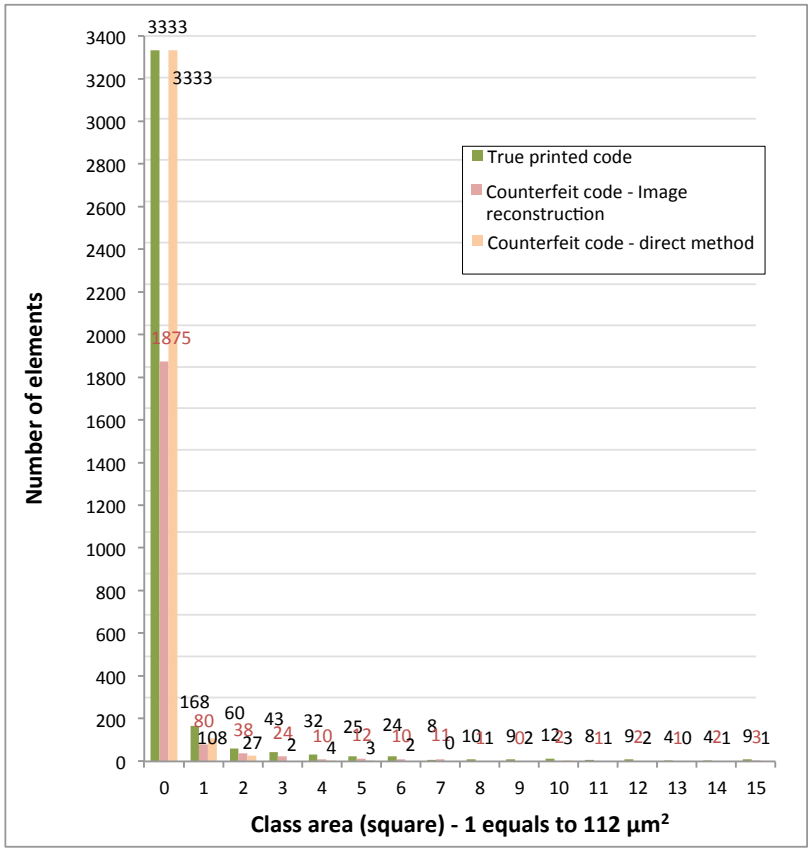

Figure 16: Size distribution histogram of a 2D code – 20 % of coverage, 42.4 µm dot, electrophotography printed on uncoated paper – comparison of the different counterfeiting strategies

4. Discussion

4.1 Case of the first print

The class area 0 corresponds to the smallest elements composing the image. It includes some elements resulting from the acquisition and pre-analysis treatment; taking into consideration that almost all the tasks have been automated, these factors are common to all the samples. Therefore, the class 0 characterizes mainly the smallest printed elements such as satellite ink drops and interferences (Table 3).

There is a sensitive difference between coated and uncoated papers: if the other parameters are identical, the number of elements in the class area 0 is 2 to 7.5 times higher for uncoated paper than for coated paper. The surface finish of the uncoated paper is less adapted to a clean printing than the coated one. These results can be explained by the lower surface state quality of the uncoated paper that exhibits a higher roughness: 6.3 compared to 0.8 µm for coated paper. Indeed, this roughness value is of the same order of magnitude than the size of the smallest dot (10.6 µm). If the printed codes were perfectly identical to the digital file, no elements would be detected in the class 0.

In addition to this raise of the class 0, it must be underlined that there are 4 to 19 times less elements in the classes 1 to 5 in the printed code than in the digital file. This criterion is also a way to discriminate the printed codes and to characterize the printing process regarding the substrate.

Besides, the same analysis made on the code printed at a 42.4 µm dot size showed that the size distribution was close to the digital file for both prints, on coated and uncoated papers. It is due to the fact that the printing resolution is four times lower than the hardware resolution. It is therefore easier to print dots or groups of dots that suffer little from dot gain and deterioration.

4.2 Case of the second print

Figure 16 shows that the size distribution of the true code is very different from the two attempts of coun-

Table 3: Number of elements in the class area 0

Process	Paper	Resolution			
		2 400 dpi (10.6 μm)	1 200 dpi (21.2 μm)	800 dpi (31.8 μm)	600 dpi (42.4 μm)
Waterless offset	Coated	108	183	214	252
	Uncoated	808	1 261	536	1 069
Conventional offset	Coated	866	-	-	-
	Uncoated	1 615	-	-	-

terfeiting. The high number of small elements (class 0), higher than 3 333 for both true and counterfeit code with the direct method, is due to the printing process. Indeed, in dry electrophotography, there are a lot of satellite particles all around the initial dot (Nguyen et al., 2013). Whatever the counterfeiting method, more elements are recorded in the classes 1 to 15 for the true code than for the counterfeit ones. The small elements have been gathered in bigger elements in the counterfeiting process.

5. Conclusions

The analysis method of the codes developed in this study allows pointing out the two main phenomena generated by the printing and then the counterfeiting:

- the appearance of very small elements – class 0 (not existing in the digital file),
- the agglomeration of the small elements to form elements of bigger size (not represented on the graphics for readability considerations).

From this study, carried out for waterless and conventional offset on coated and uncoated papers, the main conclusions can be drawn:

- for a 10.6 μm dot, printed on a coated paper, there are less elements in the class 0 for waterless offset (108) than for conventional offset (866),
- a ratio 1/2 is observed in the class 0, for a code printed on uncoated paper, for waterless offset (808) compared to conventional offset (1 615).

Regarding the attempts of counterfeiting, a method was developed to re-build the code and the results showed that the size distribution analysis developed in this project is relevant to distinguish the true from the false codes for electrophotography process.

Therefore, the suitability of the method to characterize 2D codes – original and counterfeit – regarding the printing process and the kind of substrate used was demonstrated. The next step to these promising results will be to characterize groups of dots arranged according to particular configurations and also to apply the counterfeiting method to offset-printed 2D codes. The final objective consists in plotting dot profiles for different printing processes and different printed substrate and also to establish recommendations for digital model development.

In this study, we focused attention on the development of image analysis tools to be able to process pictures with automatic procedures. The next step of our study is to develop models based on physical law, on wettability of substrates and spreading of liquids in order to characterize the deposition behavior of a particular ink regarding the substrate.

Acknowledgments

This research was supported by grants from the Agence Nationale pour la Recherche (A.N.R., France – ANR-10-CORD-019).

"LGP2 is part of the LabEx Tec 21 (Investissements d'Avenir - grant agreement № ANR-11-LABX-0030) and of the Énergies du Futur and PolyNat Carnot Institutes (Investissements d'Avenir - grant agreements № ANR-11-CARN-007-01 and ANR-11-CARN-030-01)."

"This research was made possible thanks to the facilities of the TekLiCell platform funded by the Région Rhône-Alpes (ERDF: European regional development fund)."

References

VISILOG. [online] Available at <http://www.tnpc.fr/en/visilog.html> [Accessed 13 September 2015].

Chagas, L., Reverdy-Bruas, N., Pflimlin, M. and Passas, R., 2013. Characterization of a printed 2D code by image analysis. In: Enlund, N. and Lovreček, M., eds., *Advances in Printing and Media Technology*, Chemnitz: IARIGAI, Darmstadt, Germany, 40, pp. 161–168.

Chu, C.-H., Yang, D.-N., Pan, Y.-L. and Chen, M.-S., 2011. Stabilization and extraction of 2D bar codes for camera phones, *ACM Multimedia Systems Journal*, 17(2), pp. 113–133.

DENSO WAVE*, Answers to your questions about the QR code*. [online] Available at <http://www.qrcode.com/en/> [Accessed 28 March 2013].

Halvorson, M., 2008. *Visual Basic® 2008 Etape par étape*. Microsoft® Press, 548 p.

Jotcham, R., 2005. Overview of anti-counterfeiting technologies. In: *The International Anti-counterfeiting Directory*, ICC Counterfeiting Intelligence Bureau, Barking, Essex, United Kingdom, pp. 29–32.

Lemaire, F., 2011. Data matrix adopted by French pharmaceutical industry, *European Industrial Pharmacy*, 8, pp. 14–15. [online] Available at <http://www.industrialpharmacy.eipg.eu/records/EIP8/EIP8%20Feb11%20P14.pdf> [Accessed 28 March 2013].

Nguyen, Q.T., Delignon, Y., Chagas, L. and Septier, F., 2014. Printer identification from micro-metric scale printing. In*: IEEE International Conference on Acoustic, Speech and Signal Processes*, Florence, Italy, pp. 6277–6280.

Stevenson, R., 2005. Laser marking matrix codes on PCBs. *Printed Circuit Design & Fab*, UP Media Group, 22(12) pp. 32–36. [online] Available at <http://pcdandf.com/cms/images/stories/mag/0512/0512stevenson.pdf> [Accessed 28 March 2013].

Swetake, Y., 2007. *How to create QR code*. [online] Available at <http://www.swetake.com/qr/qr1_en.html> [Accessed 28 March 2013].

Ulichney R., Gaubatz M. and Simske S., 2010. Encoding information in clustered-dot halftones. In: *The 26th International Conference on Digital Printing Technologies*, HP Laboratories, 5 p.

UNITAG, *Générateur de QR codes*. [online] Available at <http://www.unitag.fr/qrcode> [Accessed 07 February 2013].

Wang, H. and Zou, Y., 2006. 2D bar codes reading: solutions for camera phones., *International Journal of Signal Processing*, 3(3), pp. 164–170.